

Efficiency of energy transfer in a light-harvesting system under quantum coherence

Alexandra Olaya-Castro,^{1,*} Chiu Fan Lee,¹ Francesca Fassioli Olsen,¹ and Neil F. Johnson²

¹*Department of Physics, University of Oxford, Clarendon Laboratory, Parks Road, OX1 3PU, United Kingdom*

²*Department of Physics, University of Miami, Memorial Drive, Coral Gables, Miami, Florida FL 33126, USA*

(Received 15 April 2008; revised manuscript received 1 July 2008; published 12 August 2008)

We investigate the role of quantum coherence in the efficiency of excitation transfer in a ring-hub arrangement of interacting two-level systems, mimicking a light-harvesting antenna connected to a reaction center as it is found in natural photosynthetic systems. By using a quantum jump approach, we demonstrate that in the presence of quantum coherent energy transfer and energetic disorder, the efficiency of excitation transfer from the antenna to the reaction center depends intimately on the quantum superposition properties of the initial state. In particular, we find that efficiency is sensitive to symmetric and asymmetric superposition of states in the basis of localized excitations, indicating that initial-state properties can be used as an efficiency control parameter at low temperatures.

DOI: 10.1103/PhysRevB.78.085115

PACS number(s): 71.35.-y, 71.23.An, 82.37.Vb

I. INTRODUCTION

Solar energy conversion in photosynthetic bacteria relies on sophisticated light-harvesting (LH) antennae, which capture photons and then transfer the electronic excitation to a molecular complex which serves as a reaction center (RC). There charge separation takes place and chemical energy storage is initiated (e.g., see Ref. 1). Some of the harvesting complexes (LH1) and the RC are closely associated and form a core unit to ensure an efficient pathway for the transfer of excitations coming from peripheral antennae (LH2). This transfer takes only a few hundred picoseconds and is performed with extraordinarily high efficiency: most of the absorbed photons give rise to a charge separation event.¹ The precise mechanisms underlying such high efficiency remain elusive despite numerous studies on the subject.¹⁻⁵ In particular, whether quantum coherence plays any role on promoting the efficiency is still ambiguous.⁶⁻¹² Some works indicate that it will induce higher excitation-transfer rates¹⁰ while others argue that this may not necessarily be the case.¹¹ Remarkably, recent experimental and theoretical works¹³⁻¹⁵ indicate that long-lasting electronic coherence can indeed influence the excitation-transfer dynamics in photosynthetic complexes. For instance, quantum beats associated with electronic coherence in the Fenna-Matthews-Olson (FMO) complex of green sulfur bacteria, which connects a large LH to the RC has been reported by Engel *et al.*¹³ Also, coherence among electronic states of closely associated pigments in the RC of purple bacteria has been recently reported.¹⁴ Furthermore, the excitation transfer in organic dendrimers has attracted significant attention through the prospect of creating artificial photosynthetic systems.¹⁶ One of the key observations in these artificial systems is the evidence of coherent energy-transfer mechanisms. These experiments therefore open up the possibility of exploring (in detail) the interplay between quantum coherence and the efficiency of natural and artificial LH systems.

In this work we consider, as a model system, a ring-hub arrangement of interacting two-level systems representing a LH1-RC core unit as in purple bacteria¹⁷⁻¹⁹ and use the quantum jump approach^{20,21} to provide a simple picture of

how the quantum superposition properties of the initial state of the excitation relate to the efficiency of transfer from the LH1 complex to the RC, when coherent energy transfer and static disorder of single-site energies dominate. The quantum jump approach^{20,21} proves to be particularly suitable to describe excitation dynamics in this situation because the density-matrix elements can be calculated *exactly* from the *no-jump evolution*, given that there is only one excitation at most in the system and that only local dissipation rates (or charge separation rates) are assumed.^{1,5} Considering initial states as superpositions of single-site excitations, we find that the efficiency profile depends both on the symmetry properties of such superposition states and on the number of sites among which the excitation is initially delocalized. In particular, our results show a nontrivial interplay between excitation delocalization and efficiency as there can be an optimal delocalization length for which efficiency of transfer reaches a maximum and transfer time a minimum. Such behavior is robust to the presence of energetic disorder. The plan of this paper is as follows. Section II outlines the model of energy transfer at low temperatures, as well as how we use the quantum jump approach to calculate the main characteristics of the photosynthetic core. Section III discusses our results both for a toy model and for a more detailed Hamiltonian describing the LH1-RC complex.

II. COHERENT EXCITATION TRANSFER

We consider a system of M donor pigments surrounding a RC with N acceptors (see Fig. 1) described by the Hamiltonian $H=H_0+H_I$. Labeling the donors from 1 to M and the acceptors from $M+1$ to $M+N$, the single-particle Hamiltonian is $H_0=\sum_{\alpha=1}^{M+N}\epsilon_{\alpha}\sigma_{\alpha}^{+}\sigma_{\alpha}^{-}$, where ϵ_{α} is the excitation energy of pigment α and the interaction Hamiltonian reads

$$H_I = \sum_{j=1}^M \sum_{c=M+1}^{M+N} \gamma_{jc} \hat{V}_{jc} + \sum_{j=1; k>j}^M J_{jk} \hat{V}_{jk} + \sum_{c=M+1; r>c}^{M+N} g_{cr} \hat{V}_{cr}. \quad (1)$$

Here $\hat{V}_{ab}=\sigma_a^+\sigma_b^- + \sigma_b^+\sigma_a^-$ where σ^{\pm} is the Pauli operator for a two-level system representing the localized Q_y excited state

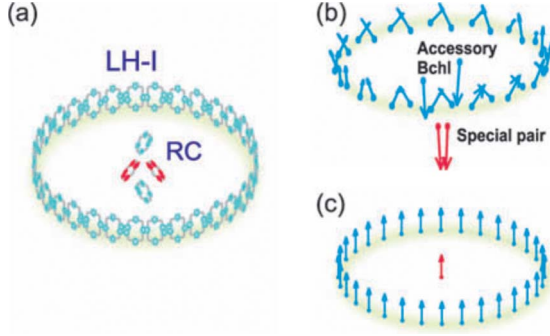


FIG. 1. (Color online) Schematic of the LH1-RC core of purple bacteria *Rhodobacter Sphaeroides*. (a) Arrangement of the 32 bacteriochlorophylls (Bchls) molecules surrounding the RC. The RC has two accessory Bchls and two acceptors forming a special pair responsible for charge separation. (b) Diagram of the induced dipole moments in (a). The arrows indicate the dipole moment directions corresponding to data taken from Hu and Schulten (Ref. 18). (c) Toy model: the RC is assumed to be a single two-level system.

of each bacteriochlorophyll a (Bchl) and γ_{jc} , J_{jk} , and g_{cr} are the donor-acceptor, donor-donor, and acceptor-acceptor couplings, respectively.¹⁷ We are interested in the low-temperature regime where static disorder dominates and dynamical effects can be neglected.²² In order to account for static disorder, we treat ϵ_α as having a random component $\epsilon_\alpha = E_\alpha + \delta E_\alpha$ where E_α is the ensemble-average value and δE_α is the energy disorder at site α given by a Gaussian distribution with zero mean and standard deviation σ . We assume that the open system dynamics is dominated by two incoherent processes: the excitation can be dissipated in a donor or it can induce charge separation at a site in the RC. Such dynamics of the photosynthetic core can be described by the Lindblad master equation ($\hbar=1$),

$$\frac{d}{dt}\rho = -i[H, \rho] + \frac{1}{2} \sum_{\alpha=1}^{M+N} [2A_\alpha \rho A_\alpha^\dagger - A_\alpha^\dagger A_\alpha \rho - \rho A_\alpha^\dagger A_\alpha], \quad (2)$$

where the commutator generates the coherent part of the evolution and the action of each operator $A_\alpha = \sqrt{2\Gamma_\alpha} \sigma_\alpha^-$ accounts for a “jump” process associated either with dissipation of excitation in a donor, i.e., $\Gamma_\alpha = \Gamma$ with $\alpha=1, \dots, M$ or with a charge separation event at an acceptor of the RC, i.e., $\Gamma_\alpha = \kappa$ with $\alpha=M+1, \dots, M+N$. Here we have assumed identical dissipation rates for the donors and identical charge separation rates for the acceptors at the RC. This formalism can be extended to include other incoherent processes.

In order to solve Eq. (2) we follow the quantum jump approach²⁰ and rewrite Eq. (2) as

$$\dot{\rho} = -i(H_{\text{cond}}\rho - \rho H_{\text{cond}}^\dagger) + \sum_{\alpha=1}^{M+N} A_\alpha \rho A_\alpha^\dagger, \quad (3)$$

with

$$H_{\text{cond}} = H - i\Gamma \sum_{j=1}^M \sigma_j^+ \sigma_j^- - i\kappa \sum_{c=M+1}^N \sigma_c^+ \sigma_c^-. \quad (4)$$

In this description, the excitation dynamics can be interpreted in terms of quantum trajectories where the system follows a *no-jump evolution* associated with the non-Hermitian Hamiltonian H_{cond} , interrupted by a single stochastic collapse of the system to its ground state in the event of either dissipation or charge separation, with probability density $p_\alpha = \text{tr}[A_\alpha \rho A_\alpha^\dagger]$. The *no-jump trajectory* conditioned on no-decay-occur is described by $\dot{\rho}_{\text{cond}}(t) = -i(H_{\text{cond}}\rho_{\text{cond}} - \rho_{\text{cond}}H_{\text{cond}}^\dagger)$. In particular, if the initial state is pure, i.e., $|\Psi(0)\rangle$, the state remains pure (but unnormalized, i.e., dissipative) in the no-jump trajectory and becomes $|\Psi_{\text{cond}}(t)\rangle = \exp(-iH_{\text{cond}}t)|\Psi(0)\rangle$.

We now demonstrate that when a single excitation is present in the photosynthetic core, the dynamics of all the density-matrix elements can be calculated exactly knowing only $\dot{\rho}_{\text{cond}}(t)$. Notice that H_{cond} preserves the number of excitations, i.e., $[H_{\text{cond}}, \mathcal{N}] = 0$ with $\mathcal{N} = \sum_{\alpha=1}^{M+N} \sigma_\alpha^+ \sigma_\alpha^-$. Hence, for a single excitation the density-matrix dynamics is restricted to the subspace of single-excitation states plus the ground state. We choose the basis given by $S = \{|0\rangle, \{|j\rangle\}, \{|c\rangle\}\}$, where $|0\rangle = |0_1 \dots 0_M; 0_{M+1} \dots 0_{M+N}\rangle$ is the state with all the pigments in their ground state and

$$|j\rangle = |0_1 \dots 1_j \dots 0_M; 0_{M+1} \dots 0_{M+N}\rangle$$

$$|c\rangle = |0_1 \dots 0_M; 0_{M+1} \dots 1_c \dots 0_{M+N}\rangle$$

are states in which only the j th donor (or c th acceptor) is excited. The labels after the semicolon in each ket refer to the acceptors at the RC. Let us denote the density-matrix elements $\rho_{kl}(t) = \langle k|\rho(t)|l\rangle$ for any pair of states $|k\rangle, |l\rangle \in S$. Notice that the second term of Eq. (3) satisfies $\langle k|A_\alpha \rho(t) A_\alpha^\dagger |l\rangle = 0$ for all states except when $|k\rangle = |l\rangle = |0\rangle$. Therefore, for single-excitation states $\dot{\rho}_{kl}(t) = \langle k|\dot{\rho}_{\text{cond}}(t)|l\rangle$, while $\dot{\rho}_{00}(t) = \sum_\alpha \langle 0|A_\alpha \rho(t) A_\alpha^\dagger |0\rangle = 2\sum_\alpha \Gamma_\alpha \langle \alpha|\rho(t)|\alpha\rangle$. Now, since $\rho(0) = \rho_{\text{cond}}(0)$, then $\rho_{00}(t) = 2\sum_\alpha \Gamma_\alpha \langle \alpha|\rho_{\text{cond}}(t)|\alpha\rangle$. This demonstrates that the dynamics of all density-matrix elements can be entirely calculated with $\rho_{\text{cond}}(t)$ and hence our claim.

A. Efficiency and transfer times

With the above formalism we can now focus on the three main features of our coherent LH1-RC core. As it is described in the review by Sener and Schulten,²³ these features are: (i) the efficiency, which is given by the probability of an excitation to be used for charge separation (as opposed to being dissipated), (ii) the average transfer time for an excitation to get trapped by the RC and (iii) the excitation lifetime after the initial absorption of a photon.

Let us denote the initial state Ψ_0 . Clearly, the probability that the excitation is still in the system at time t , i.e., *no-jump probability* is $P(t; \Psi_0) = \sum_{\alpha=1}^{M+N} \langle \alpha|\rho_{\text{cond}}(t)|\alpha\rangle$ while $w(t; \Psi_0) = \rho_{00}(t)$ is the probability density that a “jump” (charge separation or dissipation) occurs between $[t, t+dt)$ and it reads

$$w(t; \Psi_0) = 2\Gamma \sum_{j=1}^M \langle j | \rho_{\text{cond}}(t) | j \rangle + 2\kappa \sum_{c=M+1}^{M+N} \langle c | \rho_{\text{cond}}(t) | c \rangle$$

$$\equiv w_D(t; \Psi_0) + w_{\text{RC}}(t; \Psi_0). \quad (5)$$

Here $w_D(t; \Psi_0)dt$ is the probability that it is dissipated by any of the donors in $[t, t+dt)$ while $w_{\text{RC}}(t; \Psi_0)dt$ is the probability that the excitation is used for charge separation at the RC. Notice also that $w(t; \Psi_0) = -dP(t; \Psi_0)/dt$ leading to $\int_0^\infty w(t; \Psi_0)dt = 1$, which implies that the excitation will eventually either be dissipated or trapped in the RC. In particular, for pure initial states of the form $\Psi_0 = \sum_{j=1}^M b_j(0) |j\rangle + \sum_{c=M+1}^{M+N} b_c(0) |c\rangle$ with $\sum_{j=1}^M |b_j(0)|^2 + \sum_{c=M+1}^{M+N} |b_c(0)|^2 = 1$, we have $\rho_{\text{cond}}(t) = |\Psi_{\text{cond}}(t)\rangle \langle \Psi_{\text{cond}}(t)|$ with the unnormalized conditional state given by

$$|\Psi_{\text{cond}}(t)\rangle = \sum_{j=1}^M b_j(t) |j\rangle + \sum_{c=M+1}^{M+N} b_c(t) |c\rangle. \quad (6)$$

The monotonically decreasing norm of this state gives the no-jump probability $P(t; \Psi_0) = \|\Psi_{\text{cond}}(t)\|^2$ while $w_D(t; \Psi_0) = 2\Gamma \sum_{j=1}^M |b_j(t)|^2$ and

$$w_{\text{RC}}(t; \Psi_0) = 2\kappa \sum_{c=M+1}^{M+N} |b_c(t)|^2. \quad (7)$$

We therefore define the *efficiency* (η) of energy transfer to the RC as the total probability that the excitation is used in charge separation. The *transfer time* (t_f) is the average waiting time before there is a jump associated with charge separation in the RC, given that the excitation was initially in the LH1 ring. The *excitation lifetime* (τ) is the average waiting time before a jump of any kind occurs,

$$\eta = \int_0^\infty dt w_{\text{RC}}(t; \Psi_0), \quad t_f = \frac{1}{\eta} \int_0^\infty dt t w_{\text{RC}}(t; \Psi_0),$$

$$\tau = \int_0^\infty dt t w(t; \Psi_0). \quad (8)$$

III. EFFICIENCY CONTROL MECHANISMS

In the classical description,^{5,23} where incoherent Förster transfer is assumed, typical efficiencies of energy transfer tend to be near unit. This is due to a separation of the dissipation (ns) and the excitation transfer and charge separation time scales (ps). We shall shortly show that using the same parameters for single-site energies, electronic couplings, and dissipation and charge separation rates, the efficiencies obtained under coherent transfer are much lower and are strongly dependent on the initial state of the excitation. We find that the initial relative phases between localized excitation states $|j\rangle$ and the number of donors, among which the excitation is initially delocalized, can act as efficiency control mechanisms. In what follows, we first consider a simple model for which analytical solutions can be obtained and then we calculate efficiency and transfer times with the model Hamiltonian given in Refs. 17 and 18.

A. Toy model for the LH1-RC complex

The simplest model for which analytical solutions can be obtained corresponds to the RC taken as a single two-level system, i.e., $N=1$, on resonance with the $M=32$ donors in the LH1 ring [see Fig. 1(c)]. Later we shall show that the main qualitative behavior observed in this situation also applies to a model featuring the detailed structure of the LH1-RC complex in purple bacteria. We consider initial states in which the excitation is delocalized among donors, i.e., $\Psi_0 = \sum_{j=1}^M b_j(0) |j\rangle$ with $\sum_{j=1}^M |b_j(0)|^2 = 1$. The unnormalized state of Eq. (6) becomes $|\Psi_{\text{cond}}(t)\rangle = \sum_{j=1}^M b_j(t) |j\rangle + b_{M+1}(t) |M+1\rangle$ satisfying the equation $d|\Psi_{\text{cond}}(t)\rangle/dt = -iH_{\text{cond}}|\Psi_{\text{cond}}(t)\rangle$, which leads to a set of first-order coupled differential equations for the complex amplitudes $b_j(t)$ and $b_{M+1}(t)$. In the Appendix we show that when the system's dynamics is invariant with respect to exchange of donors in the antenna, one can find analytical solutions for $b_{M+1}(t)$. Let us define the effective interaction between a donor j and the rest of pigments in the LH1 ring as $\Delta_j = \sum_k J_{jk}$, i.e., the sum of all the coupling strengths between donor j and any other pigment in the LH ring. The system's dynamics is invariant with respect to donor exchange when both all donor-RC couplings are identical, i.e., $\gamma_{jc} \equiv \gamma$, and the effective interaction between a donor and the rest of pigments in the ring are also identical for all donors, i.e., $\Delta_j = \Delta$ for all j . Under these conditions, $b_{M+1}(t)$ satisfies the differential equation $\dot{b}_{M+1}(t) + X b_{M+1}(t) + Y b_{M+1}(t) = 0$ with $X = (\kappa + \Gamma + i\Delta)$ and $Y = M\gamma^2 + \kappa(\Gamma + i\Delta)$ (see details in the Appendix). For the initial condition where $b_{M+1}(0) = 0$, i.e., excitation is initially in the ring, we find

$$|b_{M+1}(t)|^2 = \mathcal{F}(t) \left| \sum_{j=1}^M b_j(0) \right|^2. \quad (9)$$

Here $\mathcal{F}(t) = 4\gamma^2 e^{-(\Gamma+\kappa)t} |\sin(\Omega t/2)|^2 / |\Omega|^2$ and Ω is the complex frequency that determines the timescale of coherent oscillations, i.e., $\Omega = \sqrt{4M\gamma^2 - (\Gamma - \kappa + i\Delta)^2}$. Note that Δ identical for all donors does not imply that the pair couplings J_{jk} need to be identical for all possible pairs. Hence, analytical solutions can be found for three different mechanisms of interaction between the donors: (i) nearest neighbors with $J_{j,j+1} = J/2$, (ii) pairwise interaction with $J_{jk} \equiv J$ for all $\langle j, k \rangle$ pairs, and (iii) dipole-dipole interactions of the form $J_{jk} = J/r_{jk}^3$ where r_{jk} is the relative position vector between the induced dipole moments of donors j and k . From Eq. (7) the probability density of having charge separation becomes $w_{\text{RC}}(t; \Psi_0) = 2\kappa |b_{M+1}(t)|^2$, then we obtain an expression for the corresponding efficiency,

$$\eta = 2\kappa |B_0|^2 \int_0^\infty \mathcal{F}(t) dt, \quad (10)$$

with $B_0 = \sum_{j=1}^M b_j(0)$. Equation (10) is the main result of this paper. It shows that the efficiency of transfer depends on the quantum coherence properties of the initial state as it becomes proportional to $|B_0|^2$, i.e., the *amplitude of probability*, and not just the probability that the excitation is initially in the LH1. Therefore, the efficiency profile is sensitive to symmetric and asymmetric superpositions of localized excitation

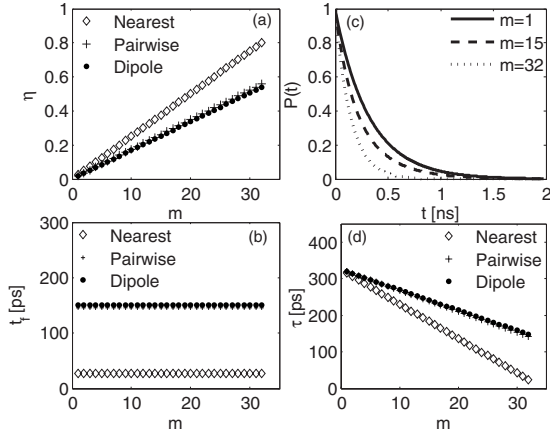


FIG. 2. Numerical results for (a) η , (b) t_f , and (d) τ versus m for the toy model with three different interaction mechanisms. For nearest-neighbor interactions (\diamond) the coupling is 100 meV, while for the pairwise (+) it is 10 meV and equals the average dipole-dipole coupling (\bullet). In each case, the donor-RC coupling γ equals 1 meV, $\Gamma=1 \text{ ns}^{-1}$, and $\kappa=4 \text{ ps}^{-1}$. (c) No-jump probability for the case of dipole-dipole interactions as a function of time and for different m values.

states $|j\rangle$, i.e., it depends on the initial relative phases between states $|j\rangle$. From Eq. (10) one can conclude that symmetric delocalized excitation states yield an increase in η while some asymmetric states could be used to limit or even prevent the transfer, i.e., $\eta=0$. Unless otherwise stated, we hence consider symmetric initial states of the form $|\Psi_m^s\rangle = (1/\sqrt{m})\sum_{j=1}^m |j\rangle$ where $m \leq M$ is the number of donors among which the excitation is initially delocalized. We denote m as the *delocalization length*. For these symmetric states $|B_0|^2 = m$ and hence $\eta \propto m$ as shown in Fig. 2(a). Figure 2(a) also shows that the efficiency gradient depends on the strength of the interaction between one donor and the rest, which is quantified by Δ . We have chosen γ to be the same for all these situations, but J has been taken to be such that $\Delta_{\text{nearest}} < \Delta_{\text{dipole}} \approx \Delta_{\text{pairwise}}$. For a fixed m , η reaches higher values in the case of nearest-neighbor couplings while it achieves similar values for dipole-dipole and pairwise interactions. According to these results, interaction among donors limits the efficiency: the stronger the effective interaction between one donor and the ring, the lower the efficiency will be. This phenomenon seems to resemble the “entanglement sharing” dynamics in the context of a central spin coupled to a spin bath.²⁴ In our case the LH1 complex can be seen as a spin bath for the RC. Dawson *et al.*²⁴ have discussed that interaction between bath spins translates to entanglement among them; since *entanglement cannot be shared arbitrarily among several particles*, interaction among spins in the bath limit entanglement between the central spin and the bath, and therefore may limit the efficiency of transfer. A discussion of efficiency and its possible relation with entanglement is beyond the scope of this paper and the work in this direction will be presented elsewhere.²⁵ Interestingly, t_f in this simple model turns out to be independent of m as can be deduced from Eq. (7). Therefore, for the symmetric initial states considered, t_f depends mainly on the mechanism of interaction as can be seen in Fig. 2(b). The decay rate of

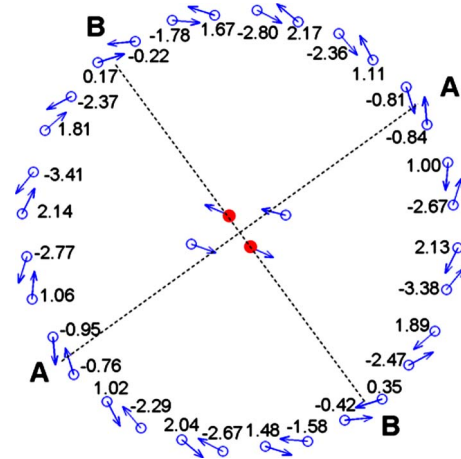


FIG. 3. (Color online) Top view of the directions of the transition dipole moments in the LH1-RC complex corresponding to the simulated data in Ref. 18. The numbers indicate total dipole-dipole interaction between individual donors and the special pair (filled circles) $\gamma_j = \sum_{c=1}^2 \gamma_{jc}$ in units of cm^{-1} . Locations A and B indicate dimmer subunits whose total coupling strengths with the special pair are maximum and minimum, respectively, i.e., $\gamma_A = -0.95 - 0.76 = -1.71$ and $\gamma_B = 0.17 - 0.22 = -0.05$.

$P(t; |\Psi_m^s\rangle)$ increases with m as shown in Fig. 2(c). Correspondingly, the excitation lifetime τ decreases as shown in Fig. 2(d). The three situations satisfy $t_f \leq \tau$, where the equality holds for the initial state in which the excitation is symmetrically delocalized among all donors.

B. Detailed model for the LH1-RC complex

We now apply the above formalism to the effective Hamiltonian for the LH1-RC interaction given in Refs. 17 and 18. In this case the RC has a special pair of Bchls responsible for the charge separation, i.e., $N=2$ acceptors and two more accessory Bchl molecules, which do not participate in the charge separation process⁴ (see Figs. 1 and 3). The effective Hamiltonian is of the form given in Eq. (1) but with certain particularities. First, the pigments at the RC are off resonance with the donors. Second, the interactions between adjacent molecules are quantified by two different constants, i.e., $J_{2j,2j+1} = \nu_1 = 806 \text{ cm}^{-1}$ and $J_{2j,2j-1} = \nu_2 = 377 \text{ cm}^{-1}$, which are derived through quantum chemical calculations.¹⁷ Third, the coupling between non-neighboring donors corresponds to a dipole-dipole interaction of the form $J_{jk} = \vec{\mu}_j \cdot \vec{\mu}_k / r_{jk}^3 - \frac{3(\vec{r}_{jk} \cdot \vec{\mu}_j)(\vec{r}_{jk} \cdot \vec{\mu}_k)}{r_{jk}^5}$, where $\vec{\mu}_j$ is the transition dipole moment of the j th donor and \vec{r}_{jk} is the relative position vector between donors j and k . The directions of μ_j have been taken from Hu *et al.*¹⁸ and top views of the dipole representation of the LH1-RC core are shown in Figs. 1(b) and 3. For the initial condition of the excitation in the LH1 complex, we consider both symmetric initial states $|\Psi_m^s\rangle = (1/\sqrt{m})\sum_{j=1}^m |j\rangle$ with total amplitude of probability $|B_0|^2 = m$ and asymmetric states $|\Psi_m^{as}\rangle = (1/\sqrt{m})\sum_{j=1}^m (-1)^j |j\rangle$ satisfying $|B_0|^2 = 0$. Since the system’s dynamics is not invariant with respect to pigment exchange, for each delocalization length m , we calculate the average efficiency $\eta_m \equiv \langle \eta \rangle$ where the average is

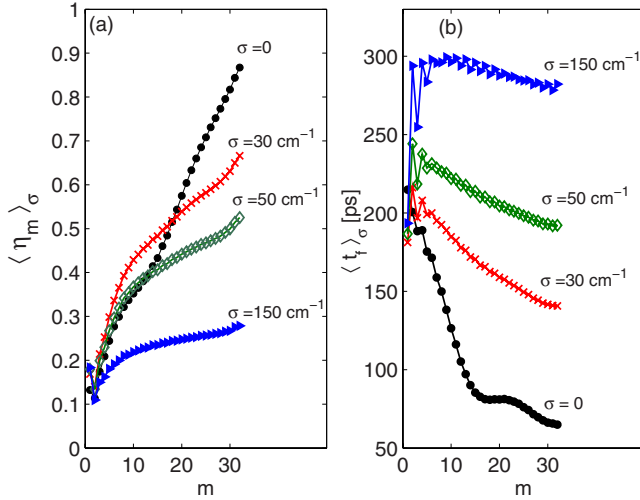


FIG. 4. (Color online) Numerical results for initial symmetric states of the form $|\Psi_m^s\rangle = (1/\sqrt{m})\sum_{j=1}^m |j\rangle$ satisfying $|B_0|^2 = m$. (a) Efficiency and (b) transfer time versus m for different σ - values. Results shown are averaged over an ensemble of 1000 aggregates for each standard deviation σ . Single-site energies and electronic couplings for the LH1-RC core have been taken from Ref. 18. For donors in the LH1 complex $E_j(0) = 12\,911 \text{ cm}^{-1}$ while for the special pair at the RC $E_c(0) = 12\,748 \text{ cm}^{-1}$ and for the accessory Bchl $E_a(0) = 12\,338 \text{ cm}^{-1}$. In all cases $\Gamma = 1 \text{ ns}^{-1}$ and $\kappa = 4 \text{ ps}^{-1}$.

taken over all possible states for which the excitation is delocalized among m consecutive donors. Also, when energetic disorder is considered for each value of standard deviation σ , the efficiency corresponds to the ensemble average over 1000 realizations of disordered H . We denote this average efficiency $\langle \eta_m \rangle_\sigma$ and the corresponding average transfer time $\langle t_f \rangle_\sigma$. An estimate of $\sigma = 30 \text{ cm}^{-1}$ for the standard deviation of the diagonal disorder distribution in the LH1 has been provided in the literature.²⁶ Therefore we have carried out calculations for σ - values ranging from 0 to 150 cm^{-1} and the results for symmetric and asymmetric initial states are shown in Figs. 4 and 5, respectively. For symmetric states and in the absence of energetic disorder, i.e., $\sigma = 0$, the behaviors of the efficiency and transfer time are very similar to that in the toy model: $\langle \eta_m \rangle_{\sigma=0}$ increases linearly with m [see Fig. 4(a)] while $\langle t_f \rangle_{\sigma=0}$ decreases [see Fig. 4(b)], achieving maximum efficiency and minimum transfer time for the fully delocalized situation. For disorder distributions corresponding to small values of σ , i.e., $\sigma \leq 50 \text{ cm}^{-1}$, there are symmetric states which exhibit efficiency improved in comparison to the situation where no disorder is considered. Such states correspond to those for which $m < 10$ as it can be seen in Fig. 4(a). However, the efficiency values are clearly decreased with increasing σ . Conversely for the asymmetric states satisfying $|B_0|^2 = 0$, the efficiency is a nonmonotonic function of m , indicating that there is an *optimal* delocalization length for which $\langle \eta_m \rangle_\sigma$ has a maximum and for which $\langle t_f \rangle_\sigma$ has a minimum as it is shown in Fig. 5. The optimal delocalization length is around $m = 8$ for zero disorder and becomes $m = 10$ for higher σ - values as it can be seen in Fig. 5(a). Such behavior is robust to the presence of energetic disorder and indeed improved as the efficiency values are larger with increasing σ . It is also worth noting that in both

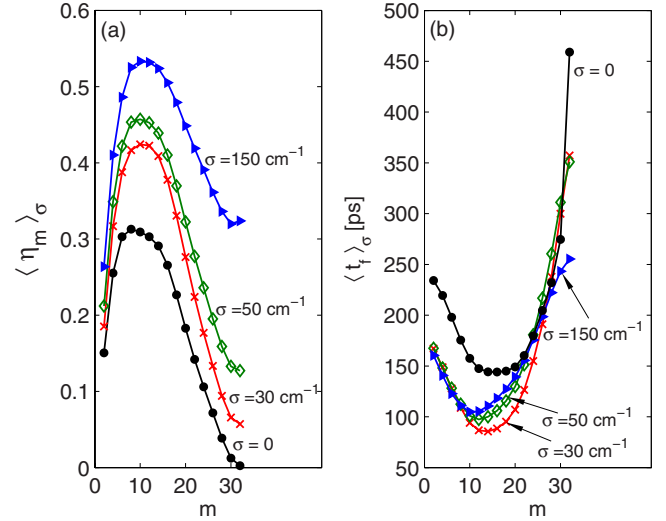


FIG. 5. (Color online) Numerical results for initial asymmetric states of the form $|\Psi_m^{as}\rangle = (1/\sqrt{m})\sum_{j=1}^m (-1)^j |j\rangle$ satisfying $|B_0|^2 = 0$. (a) Efficiency and (b) transfer time versus m for different σ - values. Results shown are averaged over an ensemble of 1000 aggregates for each standard deviation σ . Single-site energies and electronic couplings for the LH1-RC core have been taken from Ref. 18. For donors in the LH1 complex $E_j(0) = 12\,911 \text{ cm}^{-1}$ while for the special pair at the RC $E_c(0) = 12\,748 \text{ cm}^{-1}$ and for the accessory Bchl $E_a(0) = 12\,338 \text{ cm}^{-1}$. In all cases $\Gamma = 1 \text{ ns}^{-1}$ and $\kappa = 4 \text{ ps}^{-1}$.

cases (symmetric and asymmetric states), the efficiencies obtained are lower than those given by a classical calculation with rate equations derived for the same single-site energies, electronic couplings, and dissipation and charge separation rates here considered.⁵

The rich behavior exhibited in Figs. 4 and 5 has its roots in the asymmetry of the donor-RC interactions given by the presence of two acceptors at the center of the ring. The two acceptors induce a preferred axis across the ring (across the two acceptors) and a perpendicular axis to this one, such that the donor-special pair couplings, i.e., $\gamma_j = \sum_{c=1}^2 \gamma_{jc}$ are in general unequal. However, the couplings γ_j are very similar for mirror pigments with respect to the axis crossing the A points as well as for diametrically opposed Bchls, as can be seen in Fig. 3. Also, we find that the coupling between a donor and the rest of pigments in the ring is very similar for all donors, i.e., $\Delta_j \equiv \Delta \approx 1000 \text{ cm}^{-1}$. In order to understand the implications of these symmetry-breaking interactions, we can compare the zero-disorder case with our toy model but now considering site-dependent donor-RC couplings γ_j . As it is described in the Appendix, assuming $\Delta_j \equiv \Delta$ for all donors but now nonidentical γ_j , we find $b_{M+1}(t) \sim B_0^w$ where $B_0^w = \sum_{j=1}^M \gamma_j b_j(0)$ is the total *weighted amplitude of probability* that the excitation is initially in the LH1 ring. Therefore the efficiency will satisfy $\eta \sim |B_0^w|^2$ indicating that the contribution of each donor to the transfer is weighted by its coupling to the RC. For symmetric states with delocalization length m , we have $|B_0^w|^2 = (1/m)(\sum_{j=1}^m \gamma_j)^2$ while for asymmetric states with the same delocalization $|B_0^w|^2 = (1/m)(\sum_{j=1}^m (-1)^j \gamma_j)^2$. From these expressions, one can deduce that the overall maximum in the efficiency landscape is obtained when the excitation is symmetrically delocalized over the whole ring,

while the efficiency can be zero for totally asymmetric delocalized states as half the donors contribute to the transfer in the same way than the other half but with a relative π phase difference. The expression of B_0^w for the asymmetric states also justifies the fact that there will be an optimal delocalization length for which the combination of $(-1)^j \gamma_j$ values yields a maximum B_0^w as observed in Fig. 5(a). Indeed, we observe that the efficiency depends substantially on where the delocalized state is with respect to the preferred axes (results not shown). In particular, notice that the reference axes associated with the special pair indicate four dimmer subunits whose total couplings with RC are maximum and minimum as indicated, respectively, by points A and B in Fig. 3. Delocalized states that are centered around these points have, respectively, maximum and minimum efficiency (results not shown). Such dimmer positions are separated by eight to ten pigments, which can explain why $m \approx 10$ is an optimal delocalization length for asymmetric states as, in average, such length will cover a position of maximum or minimum efficiency but not both. This also explains the observed shoulder at around $m \approx 10$ for the symmetric states.

Now let us turn the attention to the efficiency improving (diminishing) effect of disorder for asymmetric (symmetric) states. This phenomenon can be explained by recalling what we learned from the toy model presented in Sec. III A: the efficiency of an initially antisymmetric state is zero due to destructive quantum interference among donors' amplitudes. This value is clearly at a local minimum in the efficiency landscape. Therefore, by adding diagonal noise to the Hamiltonian, we are in effect pushing the efficiency of the system out of this local minimum and as such the efficiency can only become more positive. Similar arguments apply for largely delocalized symmetric states (m large): a fully delocalized state achieves the best efficiency, then any noise can only have a detrimental effect. When m is small, we observe, however, that the addition of small amount of disorder can be beneficial [see Fig. 4(a)]. This behavior is the result of an interplay between two competing effects: (i) the above discussed symmetry-breaking donor-RC interactions and (ii) the fact that a small amount of disorder in the donors' energy levels can render some of them closer to the energy level of the acceptors, which will improve the forward transfer rate.

The above results suggest that efficiency can therefore be used as an indicator for coherent energy transfer. In particular, two-dimensional spectroscopy techniques, recently developed to study coherence dynamics in photosynthetic systems,^{13,14} may be used to create and probe quantum superposition initial states. For instance, an optically allowed state of LH1 is the completely delocalized asymmetric state.¹⁷ For very low values of energetic disorder and at very low temperatures, the efficiency of transfer from such state is nearly zero as shown in Fig. 5. At a slightly higher temperature, the excitation will become less delocalized and as such the efficiency would increase (cf. Fig. 5). In other words, an experiment measuring the efficiency of an LH1-RC core under various temperatures, but still within a low-temperature regime, could serve to ascertain the extent of coherence in energy transfer. Interestingly, some experimental works have indicated that in thermalized LH2 complexes the excitation may be coherently delocalized over just a few donors of the

B850 ring,²⁷ while at very low temperatures it can be fully delocalized over the whole ring.²⁸ Although no such systematic investigation has been reported on the LH1, fluorescence excitation spectra of individual LH1-RC complex of *Rps. acidophila* at 1.2 K suggests that the excitation is largely delocalized in the LH1 ring.²⁹ An estimate of the temperature T^* below, which dominant coherent excitation transfer between the LH1 and the acceptors at the RC should be expected, is given by $k_B T^* \sim \gamma_D/a$ with $a < 1/2$.³⁰ Here γ_D is the total coupling between a dimmer subunit in the LH1 ring and the special pair at the RC and a is the dimensionless constant characterizing the coupling strength between a dimmer and its environment. The ratio between the lattice reorganization energy E_{LR} and the nearest-neighbor couplings for an individual Bchl in the LH1 ring gives an approximate value for a .³¹ Then $a \sim E_{LR}/(\nu_1 + \nu_2)$, such that $k_B T^* \sim \gamma_D(\nu_1 + \nu_2)/E_{LR}$. Taking $E_{LR} = 330 \text{ cm}^{-1}$ for the LH1 complex,^{26,31} $\gamma_D = 1 \text{ cm}^{-1}$ and $\nu_1 + \nu_2 = 1183 \text{ cm}^{-1}$, we obtain $T^* \sim 10 \text{ K}$, which is larger than the temperatures at which spectroscopic properties of LH1-RC complexes have been measured.^{26,29} Hence we believe that the described quantum phenomena can be explored with current experimental expertise.

In conclusion, we have introduced the quantum jump approach to study the role of quantum coherence in the excitation transfer in photosynthetic complexes. We have shown that initial-state properties can be used to control the efficiency of transfer in multichromophoric arrangements at low temperatures. Our results open up experimental possibilities to investigate and exploit such coherent phenomena in artificial and natural systems capable of harvesting light.

ACKNOWLEDGMENTS

A.O.C. thanks Trinity College (Oxford) for their financial support. C.F.L thanks Glasstone Trust (Oxford) and Jesus College (Oxford) for their financial support. F.F.O is grateful to Conicyt (Chile).

APPENDIX: DETAILS OF THE ANALYTICAL SOLUTIONS FOR THE TOY MODEL

As described in Sec. III A, in the simplest situation where the RC is taken as a single two-level system on resonance with M donors, we are able to find analytical solutions for the probability density of having a charge separation event at the RC and, therefore, we find an analytical expression for the efficiency of transfer in this toy model [see Eq. (10)]. Here we give the details of this calculation. The unnormalized state $|\Psi_{\text{cond}}(t)\rangle$ given in Eq. (6) satisfies the relation $d|\Psi_{\text{cond}}(t)\rangle/dt = -iH_{\text{cond}}|\Psi_{\text{cond}}(t)\rangle$, which leads to the following set of first-order coupled differential equations:

$$\dot{b}_j(t) = -i\gamma_j b_{M+1}(t) - i \sum_{k \neq j}^M J_{jk} b_k(t) - \Gamma b_j(t), \quad (A1)$$

$$\dot{b}_{M+1}(t) = -i \sum_{j=1}^M \gamma_j b_j(t) - \kappa b_{M+1}(t). \quad (A2)$$

From the above equations we obtain

$$\ddot{b}_{M+1}(t) + \kappa \dot{b}_{M+1}(t) + \sum_{j=1}^M \gamma_j^2 b_{M+1}(t) = \mathcal{G}(t),$$

with

$$\mathcal{G}(t) = i\Gamma \sum_{j=1}^M \gamma_j b_j(t) - \sum_{j=1}^M \sum_{k \neq j}^M \gamma_j J_{jk} b_k(t).$$

Let us first consider the case where all donor-RC coupling are identical, i.e., $\gamma_j \equiv \gamma$ for all $j=1 \dots M$. Defining the effective coupling between one donor and the LH1 ring as $\Delta_j = \sum_{k \neq j}^M J_{jk}$ and assuming it identical for all the donors in the LH1, i.e., $\Delta_j \equiv \Delta$, we have $\mathcal{G}(t) = (i\Gamma - \Delta) \gamma \sum_{j=1}^M b_j(t)$. Now from Eq. (A2) we get $\sum_{j=1}^M b_j(t) = i\gamma^{-1} [\dot{b}_{M+1}(t) + \kappa b_{M+1}(t)]$ and thus we arrive to

$$\ddot{b}_{M+1}(t) + X \dot{b}_{M+1}(t) + Y b_{M+1}(t) = 0, \quad (\text{A3})$$

with $X = (\kappa + \Gamma + i\Delta)$ and $Y = M\gamma^2 + \kappa(\Gamma + i\Delta)$. The solutions of the above differential equation are of the form

$$b_{M+1}(t) = f(t) \sum_{j=1}^M b_j(0) + g(t) b_{M+1}(0), \quad (\text{A4})$$

with

$$f(t) = -2i\gamma e^{-Xt/2} \frac{\sin(\Omega t/2)}{\Omega},$$

$$g(t) = e^{-Xt/2} \left[\frac{(\Gamma - \kappa + i\Delta)}{\Omega} \sin(\Omega t/2) + \cos(\Omega t/2) \right],$$

and $\Omega = \sqrt{4M\gamma^2 - (\Gamma - \kappa + i\Delta)^2}$. The above solution is invariant with respect to exchange of any pair of two-level systems. It is also worth noting that the above formalism allows to find a closed expression for the collective amplitude of probability $B(t) = \sum_{j=1}^M b_j(t)$, which leads to further simplifications of this system.³²

For the case where donor-RC couplings are unequal, but Δ_j still satisfies $\Delta_j \equiv \Delta$, we obtain $\mathcal{G}(t) = (i\Gamma - \Delta) \sum_{j=1}^M \gamma_j b_j(t) + \sum_j \alpha_j b_j(t)$ with $\alpha_j = \sum_{k \neq j} (\gamma_k - \gamma_j) J_{jk}$. Given that in the LH1-RC complex mirroring pigments as well as diametrically opposed pigments in the ring have very similar donor-special pair couplings (cf. Fig. 3), we can approximate $\mathcal{G}(t)$ as $\mathcal{G}(t) \sim (i\Gamma - \Delta) \sum_{j=1}^M \gamma_j b_j(t)$. For the initial condition $b_{M+1}(0) = 0$, we again arrive to a solution for $b_{M+1}(t)$ as in Eq. (A4), i.e., $b_{M+1}(t) = f(t) B_0^w$ and we define $B_0^w = \sum_{j=1}^M \gamma_j b_j(0)$ as the total weighted amplitude of probability that the excitation is initially in the ring.

*a.olaya@physics.ox.ac.uk

¹R. J. Cogdell, A. Gall, and J. Köhler, *Q. Rev. Biophys.* **39**, 227 (2006); X. Hu, T. Ritz, A. Damjanović, F. Autenrieth, and K. Schulten, *ibid.* **35**, 1 (2002).

²H. van Amerongen, L. Valkunas, and R. van Grondelle, *Photosynthetic Excitons* (World Scientific, Singapore, 2000).

³V. May and O. Kuhn, *Charge and Energy Transfer Dynamics in Molecular Systems* (Wiley, Weinheim, 2004).

⁴T. Ritz, A. Damjanović, and K. Schulten, *ChemPhysChem* **3**, 243 (2002).

⁵T. Ritz, S. Park, and K. Schulten, *J. Phys. Chem. B* **105**, 8259 (2001).

⁶R. M. Pearlstein, *J. Chem. Phys.* **56**, 2431 (1972).

⁷R. P. Hemenger and R. M. Pearlstein, *Chem. Phys.* **2**, 424 (1973); R. P. Hemenger, K. Lakatos-Lindenberg, and R. M. Pearlstein, *J. Chem. Phys.* **60**, 3271 (1974).

⁸J. Ray and N. Makri, *J. Phys. Chem. A* **103**, 9417 (1999).

⁹P. Herman and I. Barvik, *J. Phys. Chem. B* **103**, 10892 (1999).

¹⁰S. Jang, M. D. Newton, and R. J. Silbey, *Phys. Rev. Lett.* **92**, 218301 (2004).

¹¹K. M. Gaab and C. J. Bardeen, *J. Chem. Phys.* **121**, 7813 (2004).

¹²Y. C. Cheng and R. J. Silbey, *Phys. Rev. Lett.* **96**, 028103 (2006).

¹³G. S. Engel, T. R. Calhoun, E. L. Read, T.-K. Ahn, T. Mancal, Y.-C. Cheng, R. E. Blankenship, and G. R. Fleming, *Nature (London)* **446**, 782 (2007).

¹⁴H. Lee, Y.-C. Cheng, and G. R. Flemming, *Science* **316**, 1462 (2007).

¹⁵R. van Grondelle and V. I. Novoderezhkin, *Phys. Chem. Chem. Phys.* **8**, 793 (2006).

¹⁶D. L. Andrews and D. S. Bradshaw, *J. Chem. Phys.* **121**, 2445 (2004); J. M. Lupton, I. D. W. Samuel, P. L. Burn, and S. Muka-

mel, *J. Phys. Chem. B* **106**, 7647 (2002); M. I. Ranasinghe, Y. Wang, and T. Goodson, *J. Am. Chem. Soc.* **125**, 5258 (2003).

¹⁷X. Hu, T. Ritz, A. Damjanović, and K. Schulten, *J. Phys. Chem. B* **101**, 3854 (1997).

¹⁸X. Hu and K. Schulten, *Biophys. J.* **75**, 683 (1998).

¹⁹A. Damjanović, T. Ritz, and K. Schulten, *Int. J. Quantum Chem.* **77**, 139 (2000).

²⁰H. Carmichael, *An Open Systems Approach to Quantum Optics*, Lecture Notes in Physics Vol. 18 (Springer-Verlag, Berlin, 1993).

²¹M. B. Plenio and P. L. Knight, *Rev. Mod. Phys.* **70**, 101 (1998).

²²C. Hofmann, H. Michel, M. van Heel, and J. Köhler, *Phys. Rev. Lett.* **94**, 195501 (2005).

²³M. Sener and K. Schulten, in *Energy Harvesting Materials*, edited by David L. Andrews (World Scientific, Singapore, 2005).

²⁴C. M. Dawson, A. P. Hines, R. H. McKenzie, and G. J. Milburn, *Phys. Rev. A* **71**, 052321 (2005).

²⁵F. Fassioli Olsen and A. Olaya-Castro (unpublished).

²⁶K. Timpmann, G. Trinkunas, P. Qian, C. N. Hunter, and A. Freiberg, *Chem. Phys. Lett.* **414**, 359 (2005).

²⁷G. Trinkunas, J. L. Herek, T. Polívka, V. Sundström, and T. Pullerits, *Phys. Rev. Lett.* **86**, 4167 (2001).

²⁸A. M. van Oijen, M. Ketelaars, J. Köhler, T. J. Aartsma, and J. Schmidt, *Science* **285**, 400 (1999).

²⁹M. Ketelaars, C. Hofmann, J. Köler, T. D. Howard, R. J. Cogdell, J. Schmidt, and T. J. Aartsma, *Biophys. J.* **83**, 1701 (2002).

³⁰J. Gilmore and R. H. MacKenzie, *Chem. Phys. Lett.* **421**, 266 (2006).

³¹G. Trinkunas and A. Freiberg, *J. Lumin.* **119-120**, 105 (2006).

³²A. Olaya-Castro, C. F. Lee, and N. F. Johnson, *Europhys. Lett.* **74**, 208 (2006).